Optical properties of submicrometer-size silver needles

M. J. Bloemer,* T. L. Ferrell, M. C. Buncick, and R. J. Warmack
Health and Safety Research Division, Oak Ridge National Laboratory, Oak Ridge, Tennessee 37831-6123
(Received 28 September 1987; revised manuscript received 21 December 1987)

We present results of absorbance measurements in the range of 300–900 nm on submicrometer-size solid silver needles with aspect ratios near 7:1. The needles have parallel major axes and are formed on a transparent substrate. The needles are modeled as prolate spheroids with shapes determined from electron micrographs. Absorbance spectra as a function of wavelength, polarization, and angle are compared to theoretical absorbance curves derived from electrodynamic theory.

INTRODUCTION

In this paper we present the results of absorbance measurements on large-area arrays of silver prolate spheroids produced by a novel technique. The needles have parallel major axes which aid in the analysis of the absorbance spectra. The absorbance is measured as a function of wavelength, polarization, and angle. Two distinct peaks in the absorbance spectra are attributed to surface-plasmon excitation.[1] Theoretical particle shapes, which determine peak positions in the absorbance spectra, agree favorably with shapes found from electron micrographs.

Large arrays of post structures have been investigated for a wide variety of uses—from high-density storage media for electron beam memory[2] to low-voltage field-emission sources.[3,4] Submicrometer-size silver structures are of considerable interest in the field of surface-enhanced Raman scattering (SERS).[5] Progress in SERS has been hindered by substrates that are difficult to characterize optically and/or laborious to fabricate. In some types of SERS studies silver particles are formed on the sides of etched SiO_2 posts.[6,7] Silver particles on the sides of dielectric posts have been modeled as ellipsoids (three distinct axes) and prolate spheroids (two distinct axes). A recent technique for producing leaning posts has been developed by Buncick *et al.*[8] Silver microstructures formed on the sides of leaning posts are easier to characterize since the major axes of the particles have a defined orientation. The absorbance measurements by Buncick *et al.* indicate that silver particles on posts are best modeled as ellipsoids.

Studies concerning the growth of silver needles may provide insight to filament formation in the breakdown of dielectrics. Filaments have been observed in metal-insulator-metal (MIM) structures.[9] Under high-field conditions metal filaments or trees will grow into the insulator. The filament eventually reaches the opposite electrode and provides a conducting link resulting in total breakdown. Dielectric breakdown by filament growth occurs in integrated circuits as well as high-power transmission cables.[10]

A simple technique for fabricating silver needles is described below in which silver needles can be formed over large areas (>1 cm^2) with 50–60 needles per square micrometer. Comparisons of optical-absorbance measurements and theory confirm the needles are reasonably well modeled as prolate spheroids.

THEORY

Recently, papers have been published on the calculation of optical scattering and absorption cross sections for silver oblate spheroids[11] and ellipsoids.[8] We will follow a similar treatment for prolate spheroids by employing the formalism of Ritchie *et al.*[12] The use of nonretarded electrodynamics makes the calculation tractable.

The three prolate coordinates are η, θ, and ϕ.[13] A constant value of η specifies the surface of a prolate spheroid. The angle ϕ is the azimuthal angle about the major axis of the spheroid. The coordinate θ specifies a hyperboloid where θ is the angle between the asymptote of a hyperboloid and the major axis of the prolate spheroid. The family of prolate spheroids is generated by

$$\frac{x^2+y^2}{\eta^2-1}+\frac{z^2}{\eta^2}=a^2\,, \tag{1}$$

where a is the focal length of the prolate spheroid. The coordinate η is related to the ratio R of the minor-axis length to the major-axis length by

$$R=\frac{(\eta^2-1)^{1/2}}{\eta}\,. \tag{2}$$

The extreme shapes of a prolate spheroid are a sphere and a needle.

Reference 13 gives the solutions to Laplace's equation in prolate spheroidal coordinates. To the potential outside the prolate spheroid we add a term corresponding to a time-varying, but uniform, electric field (dipole approximation). Applying the boundary conditions at the surface, we eventually find the Fourier components of the induced dipole moments to be

$$\mathbf{p}_x(\omega)=\left.\frac{-2a^3[\epsilon(\omega)-1](\eta_0^2-1)^{1/2}P'_{11}(\eta)\mathbf{E}_x(\omega)}{3[\epsilon(\omega)P'_{11}(\eta)Q_{11}(\eta_0)-P_{11}(\eta_0)Q'_{11}(\eta_0)]}\right|_{\eta=\eta_0}, \tag{3}$$

$$\mathbf{p}_y(\omega)=\left.\frac{-2a^3[\epsilon(\omega)-1](\eta_0^2-1)^{1/2}P'_{11}(\eta)\mathbf{E}_y(\omega)}{3[\epsilon(\omega)P'_{11}(\eta)Q_{11}(\eta_0)-P_{11}(\eta_0)Q'_{11}(\eta_0)]}\right|_{\eta=\eta_0}, \tag{4}$$

$$\mathbf{p}_z(\omega)=\left.\frac{a^3\eta_0[\epsilon(\omega)-1]P'_{10}(\eta)\mathbf{E}_z(\omega)}{3[\epsilon(\omega)P'_{10}(\eta)Q_{10}(\eta_0)-P_{10}(\eta_0)Q'_{10}(\eta_0)]}\right|_{\eta=\eta_0}, \tag{5}$$

where $p_{l,m}(\eta)$ and $Q_{l,m}(\eta)$ are the associated Legendre functions, $\epsilon(\omega)$ is the complex dielectric response of the particle, and $\mathbf{E}_i$ are the amplitudes of the applied field. The major axis of the prolate spheroid is oriented along the z axis. The dipole moments are related to the polarizability α_i by

$$\mathbf{p}_i=\alpha_i\mathbf{E}_i \ . \tag{6}$$

With the expressions for the induced moments, we can calculate the scattered field[14]

$$\mathbf{E}_{\text{scat}}=\frac{\omega^2 e^{ikr}}{c^2 r}[(\hat{\mathbf{n}}\times\mathbf{p})\times\hat{\mathbf{n}}] \ , \tag{7}$$

where $\hat{\mathbf{n}}$ is a unit vector in the scattered direction. Using the expressions for the scattered field, the total (scattering and absorption) cross section for the two orthogonal polarizations s and p can be written as

$$\sigma_t|_s=\frac{4\pi\omega}{c}\text{Im}(\alpha_x) \ , \tag{8}$$

$$\sigma_t|_p=\frac{4\pi\omega}{c}\text{Im}(\alpha_y\cos^2\theta+\alpha_z\sin^2\theta) \ , \tag{9}$$

where θ is the angle between the line of incidence and the major axis of the prolate spheroid.

If I_0 is the intensity incident on the spheroid, then

$$I_0=I_t+I_a+I_s \ , \tag{10}$$

where I_t, I_a, and I_s are the transmitted, absorbed, and scattered intensities, respectively. From Eq. (10) we find

$$\frac{I_t}{I_0}=1-\left[\frac{I_s}{I_0}+\frac{I_a}{I_0}\right]=1-N\sigma_t \ , \tag{11}$$

where N is the number of spheroids per unit area. In the experiment we measure the intensity that passes through the sample which includes I_t and any light that scatters into the solid angle subtended by the detector. Therefore, Eq. (11) approximates the experimental transmittance if $I_s \ll I_a$ or if most of the scattered light is not scattered

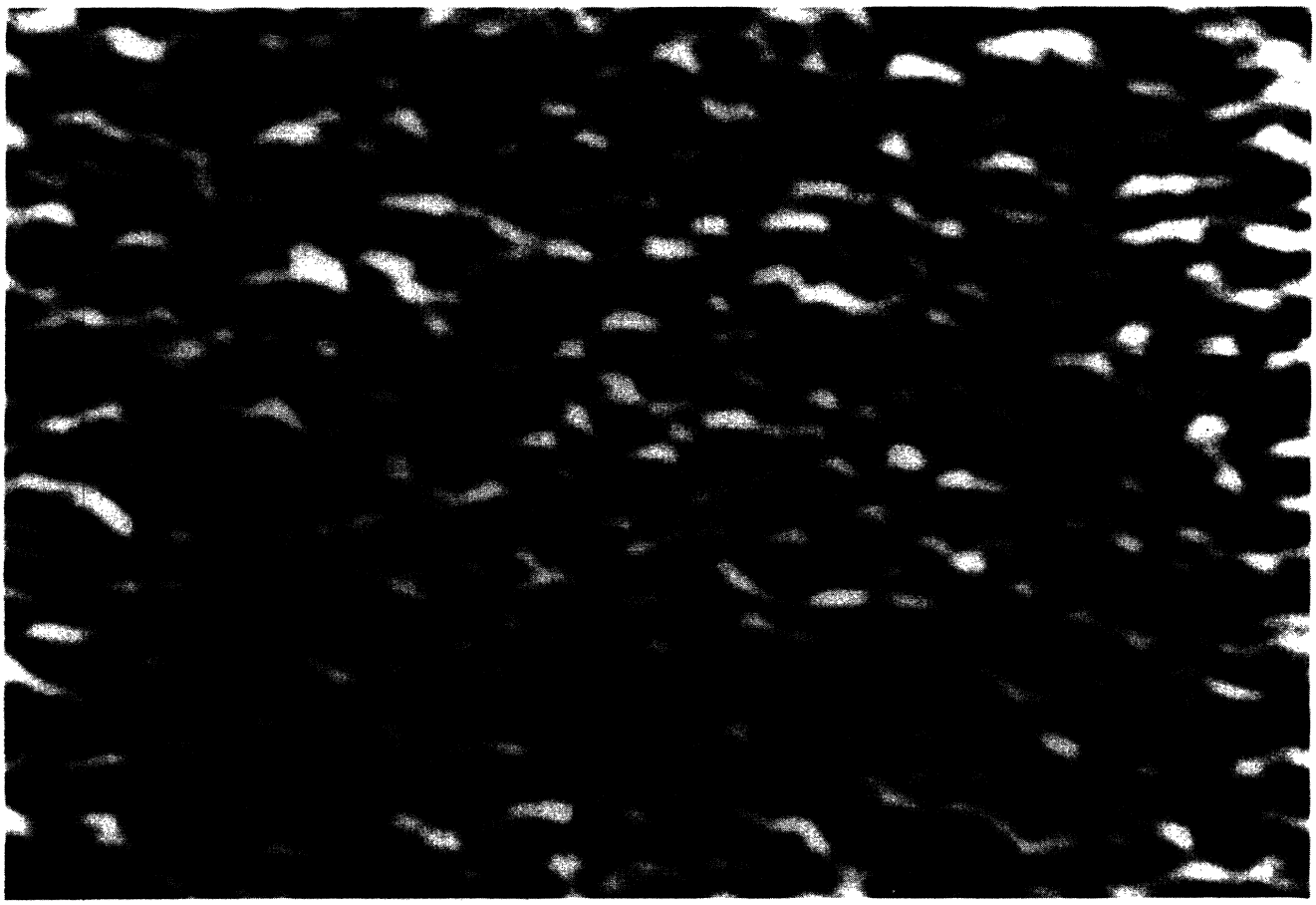

FIG. 1. Electron micrograph of a tin oxide surface. The angle of observation is 60° from the substrate normal.

into the detector. In the experiment we used a spectrophotometer to measure the absorbance

$$A = -\log_{10}(T) , \tag{12}$$

where T is the transmittance.[15]

We have not calculated the intensity of light collected by the detector due to scattering. Neglecting a component of the scattered light might lead to discrepancies when comparing absolute values of the absorbance found experimentally and theoretically.

SAMPLE PREPARATION

The growth process for silver needles requires a surface with submicrometer roughness. The substrate is mounted in the evaporation system at near grazing incidence with respect to the crucible or boat. During the evaporation, the silver begins to fill in the unshadowed areas. Once a needle sprouts, it continues to grow and maintains an approximately constant diameter. Thus, very large aspect ratios can be attained by this process of microfabrication. Short-range forces, as well as shadowing, may also be a contributing factor in the needle formation since the silver atoms pass nearly parallel to the surface.

Quartz microscope slides,[16] 12×25 mm^2, provided sturdy, transparent substrates. They were carefully cleaned before a roughness layer was deposited on the surface. Silver needles were grown successfully on two different types of roughness. Substrates were made conducting to test the effect of applied electric fields on needle formation.

It is well known that CaF_2 has a rough surface with an amplitude that depends on film thickness, at least up to some limiting thickness. A 200-nm film of CaF_2 provided suitable roughness. Next, an 80-nm silver film was deposited at normal incidence to form a good conducting layer. The final silver evaporation at grazing incidence took place at a rate of 2 nm/sec with the height of the needles being nearly equal to the total evaporation thickness. The film depth was measured by a quartz crystal thickness monitor. All evaporations took place in a cryopumped, electron beam evaporator at a pressure of 1×10^{-6} torr.

A tin oxide substrate proved to be a better choice of roughness for optical-absorbance experiments. Tin oxide is a conductor and is transparent in the visible. If it is deposited in the following manner, a hilly topography will result.

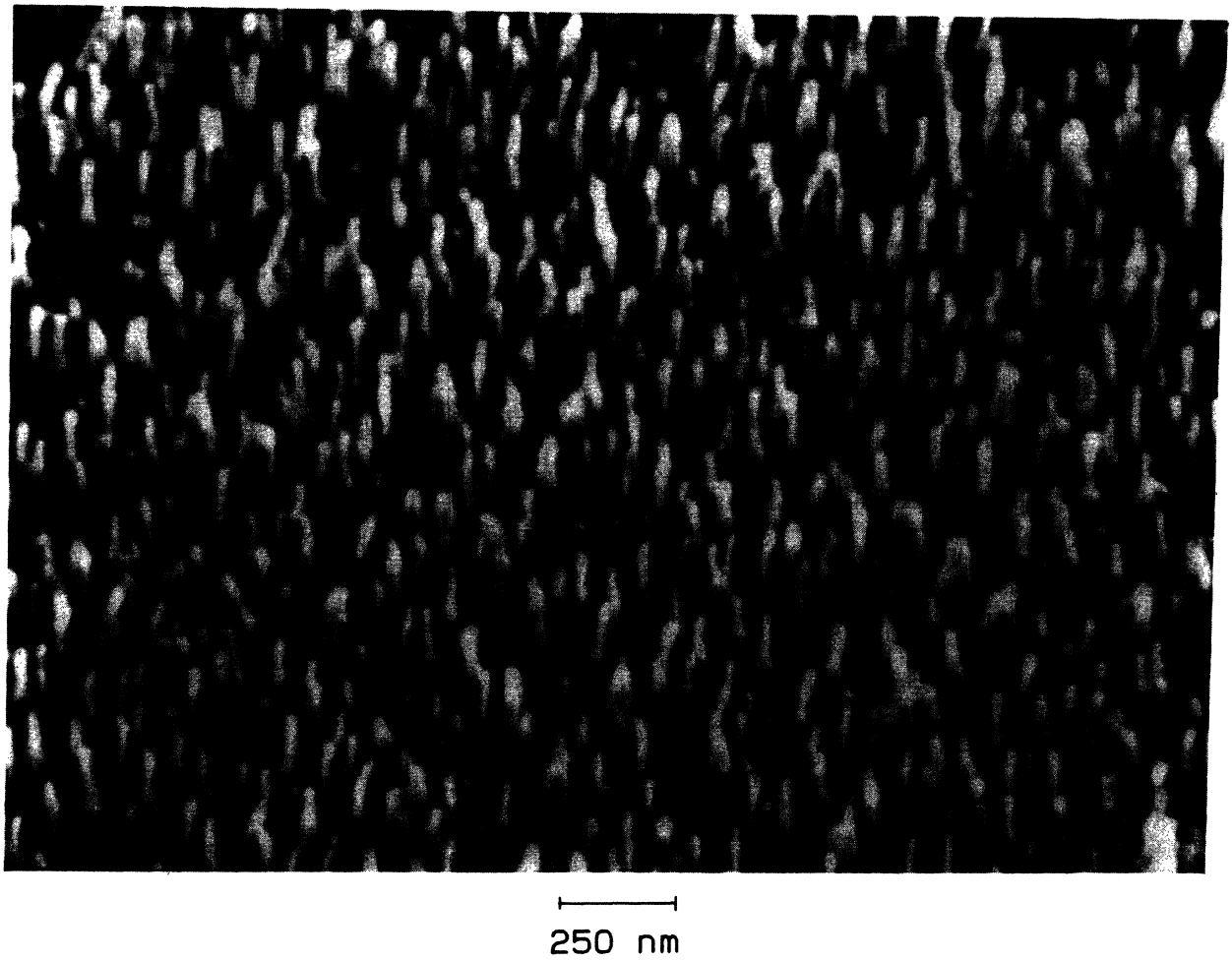

FIG. 2. Electron micrograph of solid silver posts. Observation angle is along the substrate normal (the major axes of the posts lie 60° from the substrate normal).

The quartz substrate is baked in an oven to 600 °C. Once the quartz is uniformly heated, the oven door is opened and a solution of $SnCl_4$ (in ethanol) is forced through a nozzle and sprayed onto the substrate for ~3 sec. The door is then closed and the oven turned off. The sample is allowed to cool and the process is repeated once more. Figure 1 is a scanning electron micrograph of the tin oxide surface. Micrographs of the silver-coated CaF_2 reveal similar topography.

Figure 2 is a micrograph of solid silver needles formed on a tin oxide layer. An average silver thickness of 210 nm resulted in posts approximately 200 nm tall and 30 nm across. These conditions were used to produce the needles shown in Fig. 2 and the absorbance data. The distance from crucible to substrate was 30 cm to ensure the major axes of the needles are parallel. The needle size and density are constant over the entire sample.

Micrographs at various angles seem to indicate that the needles are tilted ~60° from the substrate normal. Mounted in the evaporator, the needles lean toward the crucible. In an effort to reduce this angle, the sample was mounted in a capacitor arrangement inside the bell jar. When a bias voltage is applied to the sample, the electric field strengths are enhanced at the tips of the needles and substrate roughness. Thus, polarization forces in the direction of the applied field would tend to redirect the incident silver atoms more normal to the substrate. However, no pronounced effect on the orientation or shape of the needles resulted even for average field strengths of up to 15 000 V/cm.

RESULTS AND DISCUSSION

Absorbance measurements were obtained with a Shimadzu spectrophotometer.[17] The emitted light was polarized by Glan prisms suitable for the 300–900-nm wavelength. Employed as a reference was a quartz substrate with a tin oxide layer deposited in the same batch as the sample with needles. To account for the effect of the substrate which supports the needles, the value of the intensity of light that passes through the reference is considered to be I_0, the intensity incident on the sample. Figure 3 displays the absorbance of the reference at various angles and polarizations.

Figure 4 is the experimental absorbance of the silver needles using *s*-polarized light. For *s*-polarized light the electric field vector is perpendicular to the plane defined by the line of incidence and substrate normal. The incident angles noted in the figure are with respect to the major axis of the post and not the substrate normal (see the inset). In Fig. 4 there is only one absorbance peak for all angles since the electric field vector is always oriented along the minor axis of the needle. The needle orientation was observed in a SEM to confirm the polarization alignment illustrated in the figure inset.

The experimental absorbance for *p*-polarized light is plotted in Fig. 5. For 0°, the electric field vector is aligned along the minor axis so that only the $(l=1, m=1)$ mode is excited. As the angle with respect to the major axis of the post increases, an increasing component of the incident electric field lies along the major axis of the needles. At 90° only the long-wavelength $(l=1, m=0)$ mode is stimulated.

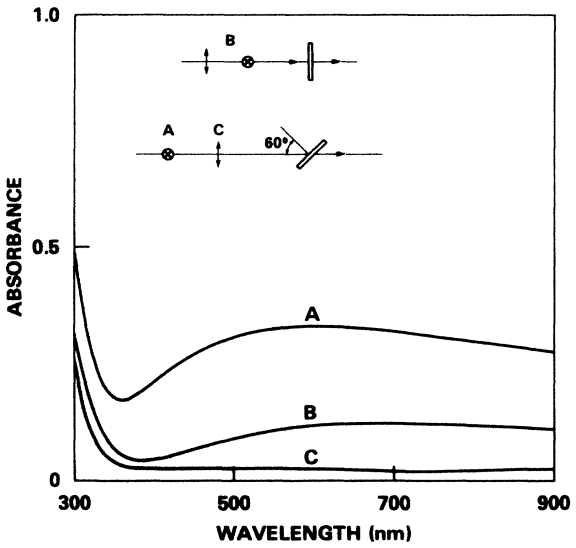

FIG. 3. Absorbance of the reference (quartz substrate with a tin oxide layer) at normal incidence and at 60° with respect to the substrate normal. Curve *A* is the absorbance of *s*-polarized light and curve *C* is for *p*-polarized light. Curve *B* was duplicated for both *s* and *p* polarizations.

For modeling the needles theoretically, a 7:1 major to minor axis ratio was chosen to be consistent with SEM micrographs. The electron micrograph illustrates that not all the needles have exactly the same aspect ratios.

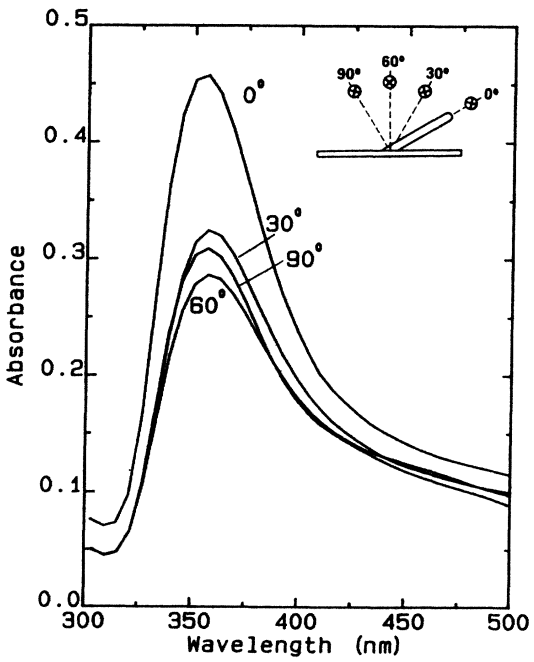

FIG. 4. Experimental absorbance of *s*-polarized light obtained from sample with needles. Incident angles are shown with respect to the major axis of the needle.

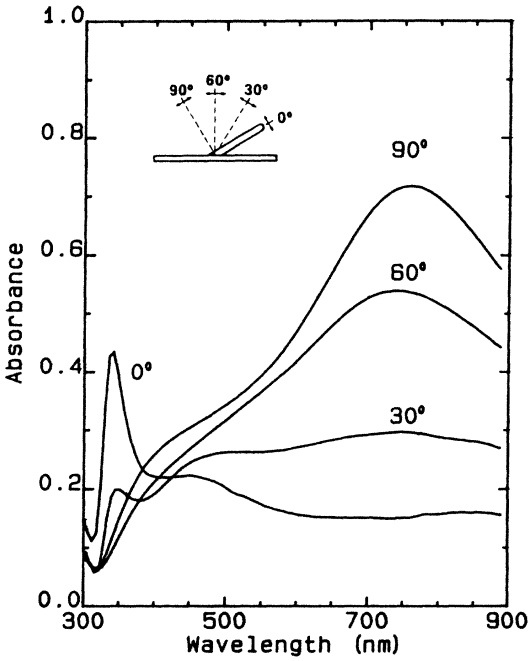

FIG. 5. Experimental absorbance of p-polarized light. Incident angles are shown with respect to the major axis of the needle.

Therefore, a Gaussian distribution of aspect ratios centered at 7:1 was included in the theoretical absorbance calculation.[18]

Figure 6 is the theoretical absorbance of p-polarized light for silver prolate spheroids with a 7:1 major to minor axis ratio. Again, all angles are with respect to the major axis of the spheroid. The peak height of the theoretical absorbance spectrum at 90° has been normalized to the corresponding experimental peak height. From the normalization we extract a value of N (the number of spheroids per unit area) through Eq. (11). We find from the micrographs that $N \simeq 55\ \mu m^{-2}$ and from Eq. (11) that $N = 10\ \mu m^{-2}$. Agreement between theory and experiment should be better if we had used a different distribution of particle shapes other than a simple Gaussian and had normalized to the area under the experimental spectra. This would tend to raise the height of the short-wavelength peak relative to the long-wavelength peak, since the resonant energy of the short-wavelength peak is only weakly dependent on a particle axis ratio.

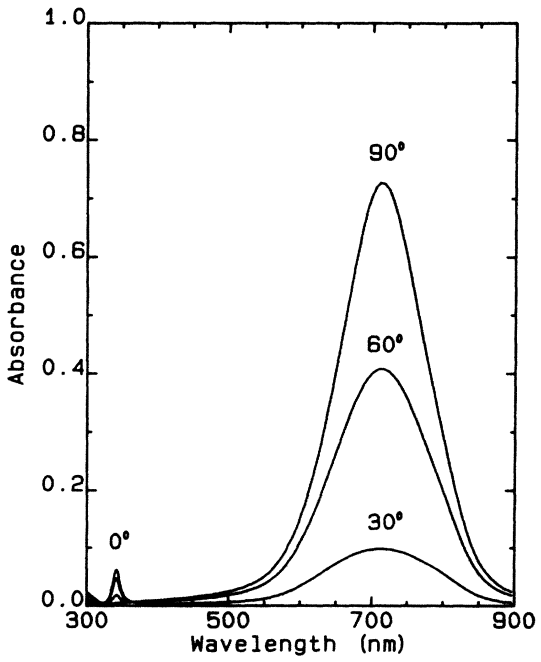

FIG. 6. Theoretical absorbance of p-polarized light for silver prolate spheroids with axis ratio of 7:1 and major axis length of 200 nm. A Gaussian shape distribution has been included.

Figure 7 depicts the theoretical absorbance of s-polarized light for all angles (solid line) and the experimental s-polarized absorbance at a 60° angle of incidence (dashed line). By normalizing the experimental and theoretical peak heights for the s-polarized spectra, we find a theoretical value of $N = 47\ \mu m^{-2}$ which is much closer to the value found from the micrographs.

The theory predicts the absorbance spectra of s-polarized light are independent of incident angle, while the experiment shows an angular dependence in peak height. We believe the disagreement between the theory and experiment in the angular dependence is due to the reflectivity of the sample increasing at a faster rate than the reflectivity of the reference. We measured the intensity of the light transmitted through the sample and

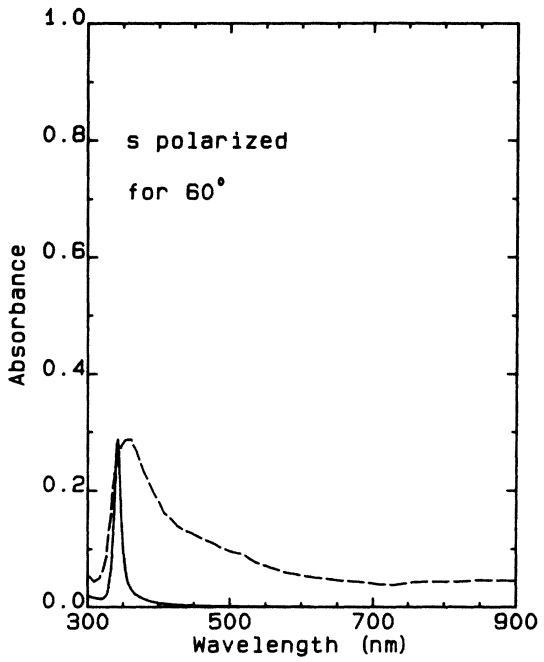

FIG. 7. Solid curve: Theoretical absorbance of s-polarized light at any incident angle. The silver prolate spheroids are modeled as having a major to minor axis ratio of 7:1 and a major axis length of 200 nm. A Gaussian distribution of shapes has been included. Dashed curve: Experimental absorbance of s-polarized light incident at 60° with respect to the major axis of the spheroid.

through a reference. This negates changes in the reflectivity of the substrate with angle but not variations in the reflectivity of the silver particles with angle. In addition, the theory neglects the substrate on which the particles reside. Therefore, the reflectivity at the silver–tin-oxide interface may also contribute to variations in peak heights.

To test this assumption, we evaporated a 5-nm mass thickness of silver onto a quartz slide at normal incidence. A brief anneal causes the silver to form oblate spheroidal particles.[11] Silver oblate spheroids have a surface plasmon resonance near 450 nm for *s*-polarized light. Measurements in our spectrophotometer show the absorbance increases with angle, while the theory outlined above, when applied to oblate spheroids, predicts no angular dependence in absorption or scattering cross sections for *s*-polarized light. Using *s*-polarized light from an argon-ion laser (457.9 nm) we measured the intensity transmitted through and reflected from the sample with silver oblate spheroids. The intensity of the transmitted beam and the reflected beam summed to a constant value for all angles of incidence. This indicates the absorption of *s*-polarized light is independent of incident angle as predicted by theory.

Other discrepancies between the theoretical and experimental curves will now be addressed. The first is the presence of a shoulder near 450 nm in the experimental *p*-polarized absorbance. This could be attributed to the very short needles which can be observed in the electron micrograph. The other possibility is the contribution of excitations of higher-order modes in the spheroid. A more exact theory than we have presented would include effects of retardation and higher-order modes which could be significant for particles of the size here.

Also, the experimental short-wavelength peaks for the orthogonal polarizations occur at slightly different wavelengths. According to theory they should be at exactly the same position. If the geometrical cross section of the needle is not perfectly circular, we could account for this shift. It is difficult to ascertain this directly from electron micrographs taken at various angles. The effect of the substrate could also result in a shift for the two polarizations.[19] The mode with its dipole oriented parallel to the substrate should be red shifted a measurable amount. The substrate should have little effect on the dipole oriented perpendicular to the substrate. Thus the *s*-polarized absorbance peak would be slightly red shifted from the corresponding short-wavelength peak in the *p*-polarized data. This is consistent with the spectra shown in Figs. 4 and 5. Other factors not considered in the theory, such as interparticle interactions, would also be expected to shift the absorbance peaks.

CONCLUSION

Optical-absorbance spectra from arrays of solid silver needles reveal two absorbance peaks. According to the theory outlined above, the absorbance peaks indicate the excitation of the $(l=1,m=0)$ and $(l=1,m=1)$ surface plasmon modes. These surface plasmon modes correspond to induced dipoles along the major and minor axes of the needles, respectively. Reasonable agreement between theoretical and experimental resonant energies result if the needles are modeled as prolate spheroids with an average 7:1 major to minor axis ratio. Electron micrographs of the needles confirm the validity of this aspect ratio. The results of this paper also indicate that the bulk properties of silver[20] can be correctly applied to submicrometer particles.

The method of needle fabrication is simple and reliable. The technique requires no etching or special equipment other than an evaporation system. Also, submicrometer needles with parallel major axes can be formed over large areas.

ACKNOWLEDGMENTS

This research was sponsored by the Office of Energy Storage and Distribution, Electric Energy Systems Program, and the Office of Health and Environmental Research, U. S. Department of Energy, under Contract No. DE-AC05-840R21400 with Martin Marietta Energy Systems, Inc. This research was supported in part by an appointment to the Postgraduate Research Training Program under Contract No. DE-AC05-760OR0033 between the U.S. Department of Energy and Oak Ridge Associated Universities.

---

*Present address: Research, Development, and Engineering Center, AMSMI-RD-RE-OP, U.S. Army Missile Command, Redstone Arsenal, AL 35898-5248.

[1]R. H. Ritchie, Surf. Sci. **34**, 1 (1973).

[2]J. A. Oro and J. C. Wolfe, J. Vac. Sci. Technol. B **1**, 1088 (1983).

[3]G. A. Kitzmann, J. Phys. (Paris) Colloq., Suppl. 3 **47**, C2-79 (1986).

[4]C. A. Spindt, C. E. Holland, and R. D. Stowell, J. Phys. (Paris) Colloq., Suppl. 12 **45**, C9-269 (1984).

[5]P. F. Liao, in *Surface Enhanced Raman Scattering,* edited by R. K. Chang and T. E. Furtak (Plenum, New York, 1982).

[6]J. P. Goudonnet, T. Inagaki, T. L. Ferrell, R. J. Warmack, M. C. Buncick, and E. T. Arakawa, Chem. Phys. **106**, 225 (1986).

[7]P. F. Liao, J. G. Bergman, D. S. Chemla, A. Wokaun, J. Melngailis, A. M. Hawryluk, and N. P. Economou, Chem. Phys. Lett. **82**, 355 (1981).

[8]M. C. Buncick, R. J. Warmack, and T. L. Ferrell, J. Opt. Soc. Am. B **4**, 927 (1987).

[9]M. J. Bloemer, J. P. Goudonnet, D. R. James, R. J. Warmack, T. L. Ferrell, E. T. Arakawa, and T. A. Callcott, in *Conference Record of the 1986 IEEE International Symposium on Electrical Insulation* (IEEE Publication Services, New York, 1986), pp. 335–338.

[10]J. Raloff, Sci. News **128**, 332 (1985).

[11]S. W. Kennerly, J. W. Little, R. J. Warmack, and T. L. Ferrell, Phys. Rev. B **29**, 2926 (1984).

[12]R. H. Ritchie, J. C. Ashley, and T. L. Ferrell, in *Electromag-*

netic Surface Modes, edited by A. D. Boardman (Wiley, New York, 1982), Chap. 3.

[13]W. R. Smythe, *Static and Dynamic Electricity,* 3rd ed. (McGraw-Hill, New York, 1968).

[14]J. D. Jackson, *Classical Electrodynamics,* 2nd ed. (Wiley, New York, 1975).

[15]Spectrophotometers are often used to measure the transmittance of liquids. The strict definition of absorbance is the negative log to base 10 of the "internal" transmittance (i.e., it refers to an absorbing medium and neglects surface losses of the container holding the liquid). In the present paper, we will refer to Eq. (12) as the absorbance with the stipulation that T is the transmittance.

[16]Esco Products, Inc., Oak Ridge, NJ 07438.

[17]Shimadzu UV-250, Shimadzu Scientific Instruments, Inc., Columbia, MD 21046.

[18]The peak positions of the theoretical absorbance spectra have a slight dependence on the specific shape distribution chosen. For a single particle with a 7:1 aspect ratio, the resonances occur at $\lambda = 741$ nm and $\lambda = 343$ nm.

[19]P. Royer, J. P. Goudonnet, R. J. Warmack, and T. L. Ferrell, Phys. Rev. B **35**, 3753 (1987).

[20]H. J. Hagemann, W. Gudat, and C. Kunz, J. Opt. Soc. Am. **65**, 742 (1975).

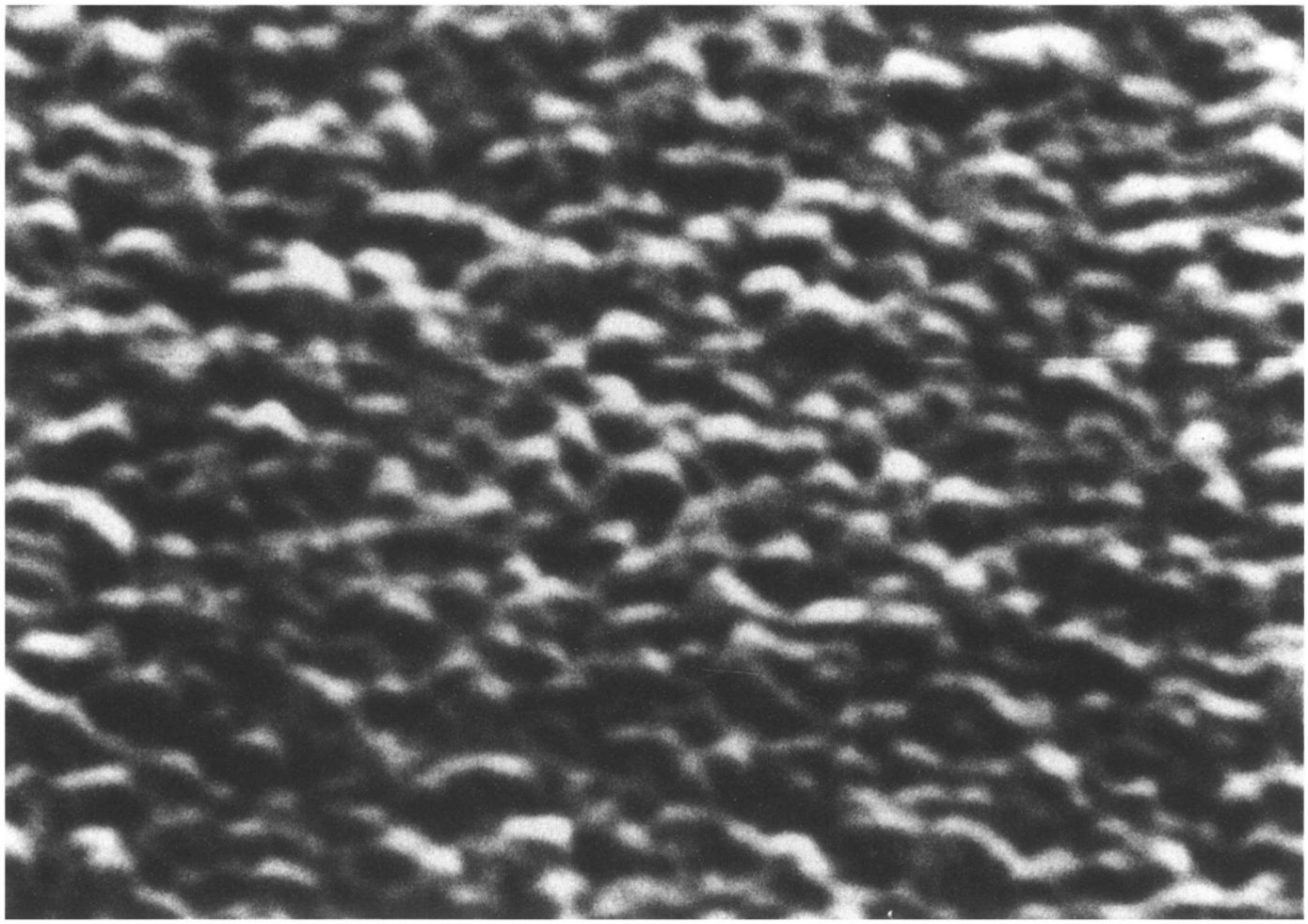

FIG. 1. Electron micrograph of a tin oxide surface. The angle of observation is 60° from the substrate normal.

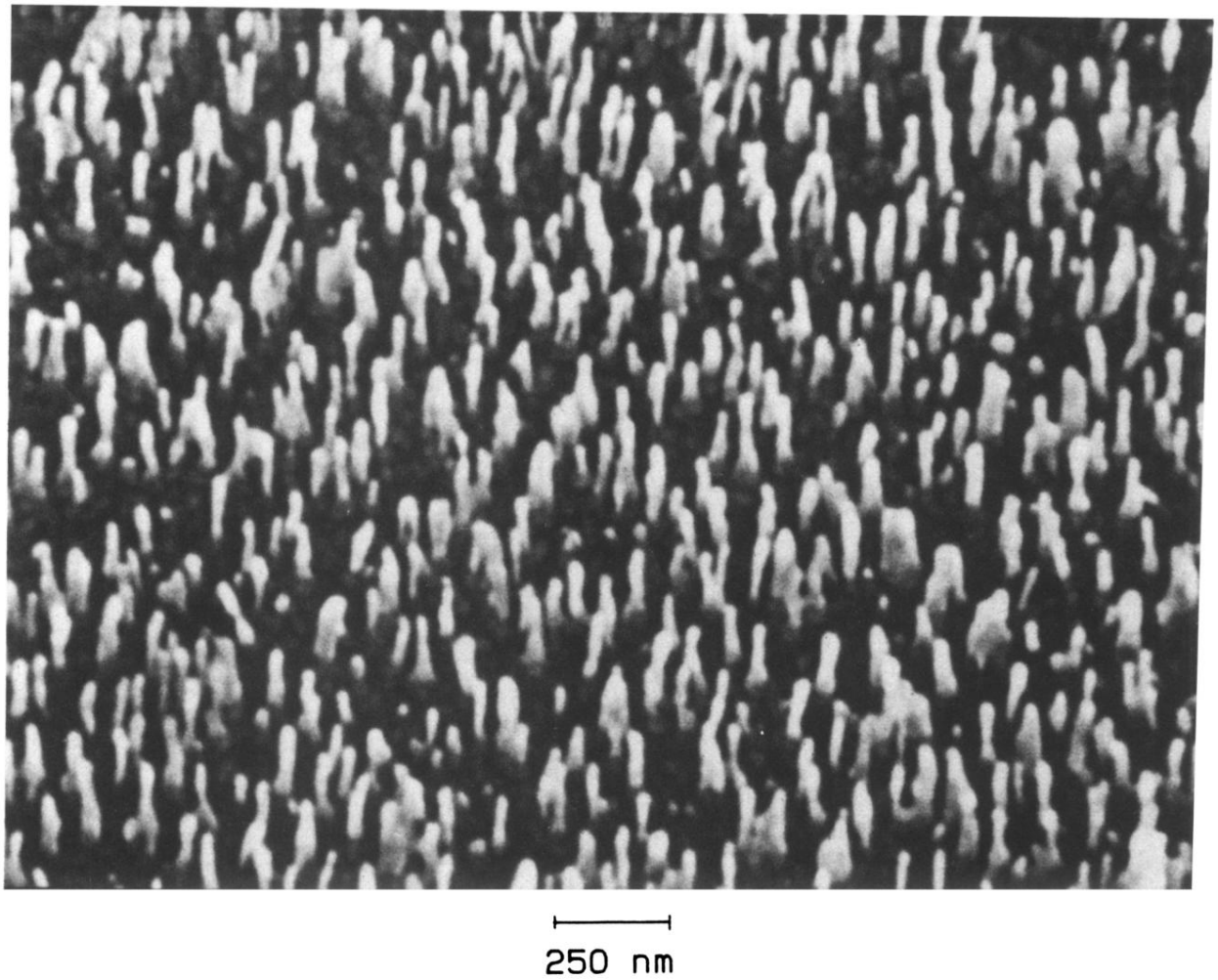

FIG. 2. Electron micrograph of solid silver posts. Observation angle is along the substrate normal (the major axes of the posts lie 60° from the substrate normal).